Synthesis, characterization and physiochemical information, along with antimicrobial studies of some metal complexes derived from an ON donor semicarbazone ligand

V.L. Siji [a], M.R. Sudarsana Kumar [a,*], S. Suma [b], M.R. Prathapachandra Kurup [c]

[a] *Department of Chemistry, M.G. College, Thiruvananthapuram 695004, Kerala, India*
[b] *Department of Chemistry, S.N. College, Chempazhanthy, Thiruvananthapuram 695587, Kerala, India*
[c] *Department of Applied Chemistry, Cochin University of Science and Technology, Kochi 682022, Kerala, India*

ARTICLE INFO

ABSTRACT

Eight new transition metal complexes of benzaldehyde-N(4)–phenylsemicarbazone have been synthesized and characterized by elemental analyses, molar conductance, electronic and infrared spectral studies. In all the complexes, the semicarbazone is coordinated as neutral bidentate ligand. ^{1}H NMR spectrum of $[Zn(HL)_2(OAc)_2]$ shows that there is no enolisation of the ligand in the complex. The magnetic susceptibility measurements indicate that Cr(III), Mn(II), Fe(III), Co(II) and Cu(II) complexes are paramagnetic and Ni(II) is diamagnetic. The EPR spectrum of $[Mn(HL)_2(OAc)_2]$ in DMF solution at 77 K shows hyperfine sextet with low intensity forbidden lines lying between each of the two main hyperfine lines. The g values calculated for the $[Cu(HL)_2SO_4]$ complex in frozen DMF, indicate the presence of unpaired electron in the $d_{x^2-y^2}$ orbital. The metal ligand bonding parameters evaluated showed strong in-plane σ bonding and in-plane π bonding. The ligand and complexes were screened for their possible antimicrobial activities.

1. Introduction

The chemistry of transition metal complexes of the semicarbazone ligands has been receiving considerable attention because of their biological relevance [1–7]. Semicarbazones are compounds with versatile structural features and can coordinate to the metal either as a neutral ligand or as a deprotonated anion. Semicarbazones exist in two tautomeric forms, keto (A) and enol (B) (Scheme 1). The coordination possibilities in semicarbazones are increased if the substituents of the aldehyde or ketone include additional donor atoms. The π-delocalization and the configurational flexibility of their molecular chain can give rise to a great variety of coordination modes [8].

Herein, we report the synthesis, spectral characterization and antimicrobial studies of eight metal complexes of benzaldehyde-N(4)–phenylsemicarbazone. The structure of the semicarbazone ligand (HL) is given (Scheme 2).

2. Experimental

2.1. Materials

The solvents used for the synthesis of semicarbazone complexes were purchased from Merck and used without further purification. N(4)-Phenylsemicarbazide (Sigma–Aldrich), benzaldehyde (Merck) were of reagent grade and were used as received. Spectrograde solvents were used for spectral recording.

2.2. Synthesis of the semicarbazone (HL)

A methanolic solution of N(4)-phenylsemicarbazide (0.151 g, 1 mmol) was refluxed with benzaldehyde (1 mmol) in methanol containing three to four drops of dilute acetic acid for 3 h (Scheme 3). On slow evaporation, colorless crystals of the compound separated out. It was filtered, washed with ether and dried over P_4O_{10} *in vacuo*. The compound was recrystallized from methanol (m.p. 176 °C, yield 75%). The elemental analysis data (Table 1) are consistent with the formula of the compound. The IR, UV–vis., ^{1}H and ^{13}C NMR data of the compound are discussed along with the complexes.

* Corresponding author. Tel.: +91 471 2592617.
  E-mail address: sudarsanmr@gmail.com (M.R.S. Kumar).

Scheme 1.

Scheme 2.

Scheme 3.

2.3. Synthesis of complexes

The complexes were prepared by refluxing 1 mmol each of appropriate salt with 2 mmol of HL in methanol for 5 h. On slow evaporation, the compounds formed were filtered, washed with methanol and dried *in vacuo* over P_4O_{10}.

2.4. Physical measurements

Analysis of carbon, hydrogen and nitrogen content of the semi-carbazone and its complexes were carried out on a Vario EL-III CHN Elemental Analyzer at the SAIF, Cochin University of Science and Technology, India. Infrared spectra were recorded on a PerkinElmer Infrared Spectrometer using KBr pellets in the range 4000–400 cm^{-1}. Electronic spectra were recorded in methanol on a Shimadzu UV-2450 UV-visible Spectrophotometer. The ^{1}H and ^{13}C NMR spectra were recorded using Bruker DRX – 500 NMR Spectrometer, with CDCl$_3$ as solvent and TMS as the standard at NIIST, Thiruvananthapuram, India. The magnetic susceptibility measurements were carried out at the Indian Institute of Technology, Roorkee, at room temperature in the polycrystalline state on a PAR model 155 Vibrating Sample Magnetometer at 5 kOe field strength. EPR spectra of complexes in solid state at 298 K and in frozen DMF at 77 K were recorded on a Varian E – 112 Spectrometer at X-band, using TCNE as marker with 100 kHz modulation frequency and 9.1 GHz microwave frequency at the SAIF, IIT, Mumbai, India. The molar conductances of the complexes in methanol solutions (10^{-3} M) at room temperature were measured using a Systronics direct reading conductivity meter.

3. Results and discussion

3.1. Analytical measurements

The colors, partial elemental analyses, molar conductivities and magnetic susceptibility values are presented in Table 1. The elemental analyses data are consistent with the molecular formula. The complexes are soluble in DMF, CHCl$_3$ and DMSO. The conductivity measurements were made in methanol solutions and all the complexes were found to be non-electrolytes. However, we could not isolate single crystals of suitable quality for X-ray diffraction studies for any of these complexes.

3.2. Magnetic susceptibilities

Room temperature magnetic susceptibility studies reveal complexes **1**, **2**, **3**, **4** and **6** to be paramagnetic. In Cr(III) and Mn(II) complexes the magnetic moments are found to be 3.29 and 5.12 B.M., respectively. The room temperature magnetic moment of Mn(II) is consistent with manganese in the +2 oxidation state,

Table 1
Colors, partial elemental analyses, molar conductivities and magnetic moments of benzaldehyde-$N(4)$–phenylsemicarbazone and its metal complexes.

Compound	Color	Composition % found (calc)			λ_m^a	μ_m^b (B.M.)
		Carbon	Hydrogen	Nitrogen		
HL	Colorless	70.24 (70.27)	5.45 (5.48)	17.72 (17.56)		
[Cr(HL)(OAc)$_3$] **(1)**	Pale blue	51.24 (51.28)	4.74 (4.74)	8.96 (8.97)	10.1	3.29
[Mn(HL)$_2$(OAc)$_2$] **(2)**	Brown	58.99 (59.01)	3.34 (3.38)	12.88 (12.91)	10.6	5.12
[Fe$_2$(HL)$_4$(SO$_4$)$_3$] **(3)**	Brown	49.53 (49.56)	3.85 (3.87)	12.68 (12.39)	8.3	3.42
[Co(HL)(OAc)$_2$] **(4)**	Pale green	51.89 (51.93)	4.63 (4.61)	10.03 (10.09)	13.3	2.04
[Ni(HL)(NO$_3$)$_2$] **(5)**	Brown	39.80 (39.85)	3.07 (3.11)	16.63 (16.60)	6.1	Diamagnetic
[Cu(HL)$_2$SO$_4$] **(6)**	Brown	52.63 (52.69)	4.81 (4.11)	13.09 (13.17)	11.3	1.82
[Zn(HL)$_2$(OAc)$_2$] **(7)**	Pale yellow	58.01 (58.05)	4.13 (4.58)	12.11 (12.69)	3.4	Diamagnetic
[Cd(HL)$_2$(NO$_3$)$_2$] **(8)**	Colorless	46.91 (47.04)	3.74 (3.67)	15.53 (15.68)	9.3	Diamagnetic

[a] Molar conductivity, 10^{-3} M methanol at 298 K.
[b] Magnetic susceptibility per metal atom.

[Cr(HL)(OAc)$_3$]

[M(HL)$_2$X$_2$]
M= Mn, Zn, Cd
X= OAc, NO$_3$

[M(HL)X$_2$]
M= Co, Ni
X= OAc, NO$_3$

[Cu(HL)$_2$SO$_4$]

[Fe$_2$(HL)$_4$(SO$_4$)$_3$]

Fig. 1. Tentative structures of the complexes.

with no significant exchange interactions between adjacent metal centers [9]. The magnetic moment value of 3.42 B.M. for the Fe(III) complex indicates a high spin low spin equilibrium [10] at room temperature. In Co(II) complex, the observed magnetic moment is much lower than that expected of four coordinate Co(II) tetrahedral complexes (4.4–4.8 B.M.) [11,12]. This suggests a possible tendency towards a square planar geometry in the complex. The Ni(II) complex is diamagnetic, consistent with a square planar structure. The room temperature magnetic susceptibility of the Cu(II) complex in the polycrystalline state is 1.82 B.M. which is very close to the spin only value of 1.73 B.M. [13] for a d^9 copper system, while the Zn(II) and Cd(II) complexes are diamagnetic.

3.3. Infrared spectra

Table 2 lists the tentative assignments of main IR bands of metal complexes for the ligand HL in the 4000–400 cm^{-1} region. The spectrum of the ligand exhibits a medium band at 3357 cm^{-1} which is assigned to ν(^{4}NH) vibration [14]. The medium band at 2917 cm^{-1} in the free ligand due to ν(^{2}NH) vibration indicates that the ligand remains in the keto form in the solid state [15,16]. The presence of this band in the complexes indicates that there is no enolisation and deprotonation of the ligand and the semicarbazone is coordinated in the neutral form. A band at 1700 cm^{-1} in the ligand is shifted to lower frequency in the com-

Table 2
Selected IR bands (cm^{-1}) with tentative assignments of benzaldehyde-N(4)–phenylsemicarbazone and its metal complexes.

Compound	ν(C=O)	ν(C=N)	ν(^{2}NH)	ν(^{4}NH)	ν(N–N)	ν(M–N)
HL	1708	1600	2917	3357	1032	–
[Cr(HL)(OAc)$_3$] (**1**)	1684	1594	3097	3371	1034	483
[Mn(HL)$_2$(OAc)$_2$] (**2**)	1686	1594	3087	3371	1040	484
[Fe$_2$(HL)$_4$(SO$_4$)$_3$] (**3**)	1683	1597	3097	3371	1043	460
[Co(HL)(OAc)$_2$] (**4**)	1683	1598	3097	3369	1045	485
[Ni(HL)(NO$_3$)$_2$] (**5**)	1685	1594	3087	3370	1045	480
[Cu(HL)$_2$SO$_4$] (**6**)	1683	1595	3099	3369	1040	485
[Zn(HL)$_2$(OAc)$_2$] (**7**)	1684	1595	3098	3371	1039	487
[Cd(HL)$_2$(NO$_3$)$_2$] (**8**)	1684	1594	2952	3371	1040	461

plexes showing the involvement of C=O oxygen in coordination. The presence of bands in the 1681–1686 cm^{-1} region for complexes supports the keto form of ligand in all the complexes. A sharp band at 1600 cm^{-1} in the semicarbazone can be attributed to the characteristic >C=N–group. This band shift slightly towards lower frequencies in the complexes [17], indicating the coordination of azomethine nitrogen to metal. It is further supported by the appearance of new bands at 460–487 cm^{-1} assignable to ν(M–N) for these complexes [18]. The ν(N–N) band of semicarbazone is observed to 1032 cm^{-1}. The increase in the ν(N–N) value in the spectra of the complexes is due to the increase in double bond character, offsetting the loss of electron density *via* donation to the metal and it is a confirmation of the coordination of the ligand through the azomethine.

In complexes **1**, **2**, **4** and **7** the asymmetric and symmetric stretching bands, corresponding to unidentate type of acetate group [18,19] are present. In complex **6**, the spectral data indicates the bidentate nature of the sulphate anion. In complex **3**, the ν_1 and ν_2 vibrations, observed as weak bands at 945 and 465 cm^{-1}, suggest the bridged bidentate [20] nature of sulphate anion in the complex. The symmetry of the sulphate is reduced to C$_{2V}$ when it functions as a bidentate ligand in the complex. The ν_3 vibrations are observed at 1080, 1143 and 1230 cm^{-1}, while the ν_4 vibrations are observed near 613 and 507 cm^{-1}. In complexes **5** and **8**, two strong bands at 1240 and 1380 cm^{-1} with a separation of 140 cm^{-1} corresponding to ν_1 and ν_4 and a medium band at 1040 cm^{-1} corresponding to ν_2 of the nitrate group indicate the presence of terminal monodentate nitrate group [18]. ν_3, ν_5 and ν_6 are observed at 748, 720 and 882 cm^{-1}, respectively [21]. The tentative structures of the complexes are given in Fig. 1.
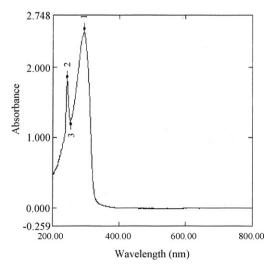
3.4. Electronic spectra

Electronic spectral data of the semicarbazone and its complexes in methanol solutions are summarized in Table 3. The $\pi \to \pi^*$ transition band in the complexes have shown a bathochromic shift due to the donation of a lone pair of electrons to the metal and hence the coordination of azomethine nitrogen. The peak due to $n \to \pi^*$ transition is associated with azomethine linkage. These bands are slightly shifted upon complexation [22]. The charge transfer bands are observed ~25,000 cm^{-1} [23] and their broadness can be explained as being due to the combination of O → M and N → M LMCT transitions. The spectra of the complexes **1**, **2**, **3**, **4** and **6** exhibit weak d–d bands in the range 13, 700–16, 670 cm^{-1} [24,25]. Representative spectrum of the semicarbazone ligand HL is presented in Fig. 2.

3.5. ^{1}H NMR spectra

The ^{1}H NMR spectrum of the compound HL and its assignments are shown in Fig. 3. A sharp singlet, which integrates as one hydrogen at δ = 9.51 ppm is assigned to the proton attached to the nitrogen atom N(2). Another singlet at δ = 7.85 ppm is assigned to the proton attached to nitrogen atom N(4). The low
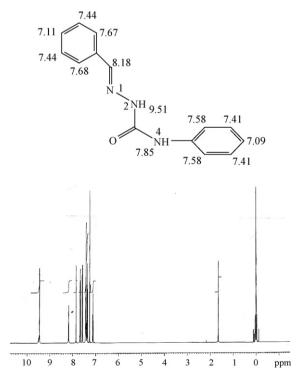

Fig. 2. Electronic spectrum of ligand HL.

Fig. 3. ^{1}H NMR spectrum of ligand HL.

Table 3
Electronic spectral assignments (cm^{-1}) of benzaldehyde-N(4)–phenylsemicarbazone and its metal complexes.

Compound	$\pi-\pi^*$	$n-\pi^*$	LMCT	d–d
HL	41,150	34,070	–	–
[Cr(HL)(OAc)$_3$] (**1**)	41,320	39,600	23,390	15,650
[Mn(HL)$_2$(OAc)$_2$] (**2**)	41,320	39,840	22,680	13,470
[Fe$_2$(HL)$_4$(SO$_4$)$_3$] (**3**)	48,310	39,060	26,040	16,670
[Co(HL)(OAc)$_2$] (**4**)	41,490	39,680	22,830	13,700
[Ni(HL)$_2$(NO$_3$)$_2$] (**5**)	41,150	39,530	26,250	–
[Cu(HL)$_2$SO$_4$] (**6**)	47,620	45,450	24,940	14,630
[Zn(HL)$_2$(OAc)$_2$] (**7**)	47,170	40,000	30,390	–
[Cd(HL)$_2$(NO$_3$)$_2$] (**8**)	39,060	37,740	31,750	–

field position of –N(4)H can be attributable to the deshielding caused by phenyl group. This downfield shift also explained the H-bonding interaction with nitrogen atom N(1). Hydrogen bonding decreases the electron density around the proton and thus moves the proton absorption to a lower field. Absence of any coupling interaction by N(2)H and N(4)H protons due to lack of availability of protons on neighbouring atoms render singlet peaks for the imine protons. The ligand does not show any peak attributable to –OH proton indicating that it exists in the keto form. IR spectral data are also in confirmity with these observations. A signal at $\delta = 8.18$ ppm is assigned to –CH=N– proton. The more downfield shift of–CH=N–can be attributed to the increased charge density on N(1) resulted by its hydrogen bonding to N(4)H and also due to electronic effect of the adjacent electronegative nitrogen. Aromatic protons of both phenyl rings appear with in the range 7.09–7.68 ppm with coupling constant 7 Hz.

The ^{1}H NMR spectrum of Zn(II) complex is shown in Fig. 4. A singlet at $\delta = 10.11$ ppm is assigned to the proton attached to the nitrogen atom N(2). Another singlet at $\delta = 7.88$ ppm is assigned to the N(4) proton. The presence of the signal due to N(2)H in the Zn(II) complex indicates that there is no enolisation of ligand in the complex. The spectrum of the complex shows a sharp singlet which integrate as one hydrogen at $\delta = 8.20$ ppm corresponds to –CH=N– present in semicarbazone moiety. In the ^{1}H NMR spectrum of ligand, a strong signal due to –CH=N– of ligand undergoes downfield shift on complexation, indicating the participation of azomethine nitrogen on bonding. The resonance for the two C$_6$H$_5$– groups appear as multiplets with in the range 7.08–7.67 ppm with coupling constant 7 Hz.

3.6. ^{13}C NMR spectrum

The ^{13}C NMR spectrum provides direct information about the carbon skeleton of the semicarbazone ligand HL. Assignment of

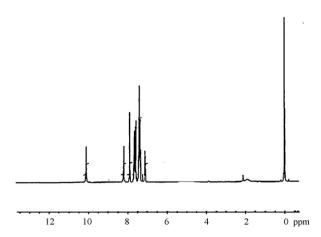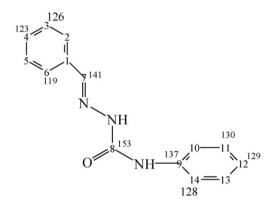different resonant peaks to respective carbon atoms is presented in Fig. 5. There are 9 unique carbon atoms in the molecule which give a total of 9 different peaks in the ^{13}C NMR spectrum. The C(8) carbon atom resonance is observed farthest downfield at $\delta = 153.61$ ppm resultant of the conjugative effect of the –N(1)–N(2)–CO–N(4)–semicarbazone skeleton. The protonated carbon atom at C(7) showing more downfield shift in the spectrum ($\delta = 141.78$ ppm), due to an increase in electron density resulting from the presence of electronegative atom and π electron delocalization on the C(7)=N(1) bond. In N(4) phenyl ring the C(9) carbon atom adjacent to more electronegative nitrogen atom N(4) are shifted farther downfield of $\delta = 137.84$ ppm when compared to the neighbouring carbon atoms. The N(4) phenyl resonances are C(9), 137.84 ppm; C(10) and C(14), 128.79 ppm; C(11) and C(13), 130.02 ppm; C(12), 129.02 ppm. Aromatic carbons of the benzaldehyde ring are observed C(1), 133.66 ppm; C(2) and C(6), 119.68 ppm; C(3) and C(5), 126.94 ppm; C(4), 123.54 ppm.
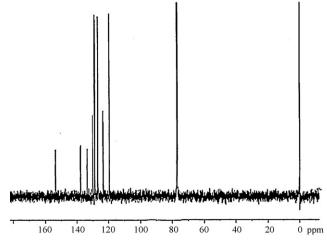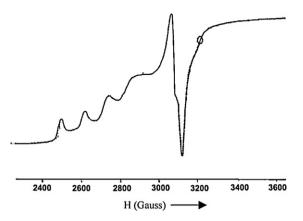

Fig. 4. ^{1}H NMR spectrum of [Zn(HL)$_2$(OAc)$_2$].

Fig. 5. ^{13}C NMR spectrum of HL.

Fig. 6. EPR spectrum of [Cu(HL)$_2$SO$_4$] in DMF solution at 77 K.

3.7. EPR spectrum of the Cu(II) complex

The EPR spectrum of the Cu(II) complex in the polycrystalline state at 298 K and in DMF at 77 K (Fig. 6) were recorded in the X-band using 100 kHz field modulation and the g factors were quoted relative to the standard marker DPPH (polycrystalline state, 298 K, $g = 2.0036$) and TCNE (DMF, 77 K, $g = 2.00277$). The EPR parameters of the copper(II) complex are presented in Table 4.

The EPR spectrum of the copper complex in the polycrystalline state (298 K) and in DMF (77 K) show typical axial behaviour with slightly different $g_{||}$ and $g_\perp$ values. The geometric parameter G, which is a measure of the exchange interaction between the copper centers in the polycrystalline compound, is calculated using the equation $G = (g_{||} - 2.0023)/(g_\perp - 2.0023)$ for axial spectrum. If $G < 4$, considerable exchange interaction is indicated in the solid complex [26]. If $G > 4$, the exchange interaction is negligible [27]. For the complex [Cu(HL)$_2$SO$_4$], the $g_{||} > g_\perp > 2.0023$ and G value is 2.98 are consistent with a $d_{x^2-y^2}$ ground state.

The EPR spectrum of the complex in the DMF solutions at 77 K is axial with four hyperfine lines in the parallel regions. For the spectra of the complex in frozen DMF, the $g_{||} > g_\perp$ values rules out the possibility of trigonal bipyramidal structures for which $g_\perp > g_{||}$ is expected. The EPR parameters $g_{||}, g_\perp, g_{av}, A_{||}$ (Cu) and the energies of d–d transition were used to evaluate the bonding parameters. α^2, β^2 and γ^2, which may be regarded as measures of the covalency of the in-plane σ bonds, in-plane π bonds and out-plane π bonds, respectively. The value of in-plane sigma bonding parameter α^2 was estimated from the following expression:

$$\alpha^2 = \frac{-A_{||}}{0.036} + (g_{||} - 2.00277) + \frac{3}{7}(g_\perp - 2.00277) + 0.04$$

The orbital reduction factors $K_{||} = \alpha^2\beta^2$ and $K_\perp = \alpha^2\gamma^2$ were calculated using the following expressions [28]:

$$K_{||}^2 = \frac{(g_{||} - 2.00277)E_{d-d}}{8\lambda_0}$$

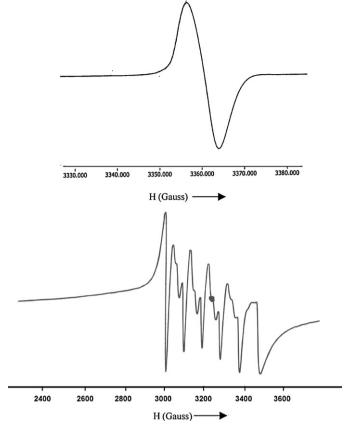$$K_\perp^2 = \frac{(g_\perp - 2.00277)E_{d-d}}{2\lambda_0}$$

Fig. 7. EPR spectra of [Mn(HL)$_2$(OAc)$_2$] in polycrystalline state at 298 K and DMF at 77 K.

where λ_0 is the spin orbit coupling constant and has the value $-828\,\text{cm}^{-1}$ for a Cu(II) d^9 system.

Hathaway [29] has pointed out that for pure σ bonding $K_{||} \approx K_\perp \approx 0.77$ and for in-plane π-bonding, $K_{||} < K_\perp$, while for out-of-plane π-bonding $K_\perp < K_{||}$. In all the complexes, it is observed that $K_{||} < K_\perp$ which indicates the presence of significant in-plane π-bonding. Furthermore α^2, β^2 and γ^2 have values less than 1.0, which is expected for 100% ionic character of the bonds and become smaller with increasing covalent bonding. Therefore the evaluated values of α^2, β^2 and γ^2 of the complexes are consistent with both in-plane σ and in-plane π-bonding. The fact that the $g_{||}$ values are less then 2.3 is an indication of significant covalent character to the M–L bond [13,30].

3.8. EPR spectrum of the Mn(II) complex

The X-band EPR spectra of manganese complex in the polycrystalline state at 298 K and DMF at 77 K are given in Fig. 7. The solid state EPR spectrum of the manganese complex at 298 K is characterized by broad signal with g value of 2.003. The signal of the spectrum observed is broadened due to dipolar interaction and a random orientation of Mn^{2+} ions. In the spectrum from DMF solutions at 77 K, a hyperfine sextet is observed with g value 2.001

Table 4
EPR parameters of Cu(II) complex in polycrystalline state at 298 K and DMF solution at 77 K.

Compound	Polycrystalline state (298 K)				DMF solution (77 K)								
	$g_{||}$	$g_\perp$	g_{av}	G	$g_{||}$	$g_\perp$	g_{av}	$A_{||}$[a]	α^2	β^2	γ^2	$K_{||}$	$K_\perp$
[Cu(HL)$_2$SO$_4$]	2.181	2.062	2.102	2.98	2.295	2.088	2.157	166.67	0.86	0.92	0.99	0.80	0.86

[a] Expressed in units of cm^{-1} multiplied by a factor of 10^{-4}.

and A_{iso} value 96 G, respectively. The six hyperfine lines are due to the interaction of the electron spin with nuclear spin (^{55}Mn, $I = 5/2$). In addition to this, a pair of low intensity forbidden lines lying between each of the two main hyperfine lines with an average spacing of 23 G is observed corresponding to $\Delta m_I = \pm 1$ [31]. The forbidden lines in the spectrum arise due to the mixture of the nuclear hyperfine levels by the zero-field splitting factor of the Hamiltonian [32,33].

The observed g value is very close to the free electron spin value of 2.0023, suggestive of the absence of spin orbit coupling in the ground state. The A_{iso} values are consistent with an octahedral coordination [34], since A_{iso} in tetrahedral sites is 20–25% lower than in octahedral sites. The A_{iso} values are some what lower than pure ionic compounds, which reflect the covalent nature of the metal–ligand bond in the complex.

3.9. Antimicrobial studies

All complexes (**1**–**8**) along with their parent semicarbazone ligand were screened against five bacterial cultures *viz.*, *E. coli* MTCC 585, *Salmonella typhi* MTCC 734, *Proteus vulgaris* MTCC 1771, *Enterobacter aerogenes* MTCC 2990, *Bacillus megaterium* MTCC 2248 and two fungal cultures *viz.*, *Aspergillus niger* MTCC 281 and *Candida albicans* MTCC 3018. The antimicrobial properties were determined by the standard disc diffusion method [35]. The viable bacterial cells were swabbed onto MHA plates and fungal spores onto RBA plates. The compounds were dissolved in chloroform to a final concentration of 0.1%. The petri-plates were incubated for 24 h for bacterial cultures and 76 h for fungal cultures. The activity of the compounds was counted by measuring diameter of the inhibition zone in millimeters. Test substances which produce a zone of inhibition of diameters 9 mm or more are regarded as positive, *i.e.* having constructive antimicrobial activity, while in those cases where the diameter is below 9 mm, the bacteria are resistant to the sample tested and the sample is said to have no antimicrobial activity.

Benzaldehyde-*N*(4)–phenylsemicarbazone was found to be inactive against bacteria and fungi. Out of five bacterial cultures tested, [Fe$_2$(HL)$_4$(SO$_4$)$_3$] exhibited wide spectrum of activity against *E. coli* MTCC 585 (10.5 mm), *Salmonella typhi* MTCC 734 (7.5 mm), *Proteus vulgaris* MTCC 1771 (10.5 mm) and [Ni(HL)(NO$_3$)$_2$] was found to be active against *E. coli* MTCC 585 (9 mm) and *Proteus vulgaris* MTCC 1771 (9 mm) and [Cu(HL)$_2$SO$_4$] was found to be active against *Salmonella typhi* MTCC 734 (18 mm). It is known that the chelation tends to increase the antibacterial activity of the ligand. It is observed that, in a complex, the positive charge of the metal is partially shared with the donor atoms present in the ligand, and there may be π-electron delocalization over the whole chelate. This increases the lipophilic character of the metal chelate and favors its permeation through the lipid layer of the bacterial membranes [36]. From two fungal cultures tested, only [Cu(HL)$_2$SO$_4$] exhibited activity against *Candida albicans* MTCC 3018 giving a zone of inhibition of 18 mm. The mode of action may involve the formation of a hydrogen bond through the azomethine nitrogen atom with the active centers of the cell constituents, resulting in interference with the normal cell process [37].

References

[1] J.R. Dimmock, R.N. Puthucode, J.M. Smith, M. Hetherington, J.W. Quail, U. Pugazhenthi, J. Lechler, J.P. Stables, J. Med. Chem. 39 (1996) 3984–3997.
[2] D.X. West, A.E. Liberta, S.B. Padhye, R.C. Chikate, P.B. Sonawane, A.S. Kumbhar, R.G. Yerande, Coord. Chem. Rev. 123 (1993) 49–71.
[3] I. Haiduc, C. Silvestru, Coord. Chem. Rev. 99 (1990) 253–296.
[4] S. Dutta, F. Basuli, S.M. Peng, G.H. Lee, S. Bhattacharya, New J. Chem. 26 (2002) 1607–1612.
[5] F. Basuli, S.M. Peng, S. Bhattacharya, Inorg. Chem. 40 (2001) 1126–1133.
[6] I. Pal, F. Basuli, T.C.W. Mak, S. Bhattacharya, Angew. Chem. Int. Ed. 40 (2001) 2923–2925.
[7] F. Basuli, S.M. Peng, S. Bhattacharya, Inorg. Chem. 39 (2000) 1120–1127.
[8] J.S. Casas, M.S. Garcia-Tasende, J. Sordo, Coord. Chem. Rev. 209 (2000) 197–261.
[9] M. Devereux, M. McCann, V. Leon, R. Kelly, D. Osheaa, V. McKee, Polyhedron 22 (2003) 3187–3194.
[10] B.S. Garg, M.R.P. Kurup, S.K. Jain, Y.K. Bhoon, Synth. React. Inorg. Met. Org. Chem. 28 (1998) 1415–1426.
[11] J.R. Anacona, Gladys Da Silva, J. Chil. Chem. Soc. 50 (N2) (2005) 447–450.
[12] J.C. Bailar, H.J. Emeleus, R. Nyholm, A.F. Trotman, Dickenson in Comprehensive Inorganic Chemistry, Pergamon Press, New York, 1975.
[13] U.L. Kala, S. Suma, M.R.P. Kurup, S. Krishnan, R.P. John, Polyhedron 26 (2007) 1427–1435.
[14] A.K. El-Sawaf, D.X. West, F.A. El-Saied, R.M. El-Babnasawy, Transit. Met. Chem. 23 (1998) 649–655.
[15] Y.-P. Tian, W.-T. Yu, C.-Y. Zhao, M.-H. Jiang, Z.-G. Cai, H.-K. Fun, Polyhedron 21 (2002) 1217–1222.
[16] R.P. John, A. Sreekanth, M.R.P. Kurup, H.-K. Fun, Polyhedron 24 (2005) 601–610.
[17] B.S. Garg, M.R.P. Kurup, S.K. Jain, Y.K. Bhoon, Transit. Met. Chem. 13 (1988) 92–95.
[18] K. Nakamoto, Infrared and Raman Spectra of Inorganic and Coordination Compounds, Part B, 5th ed., Wiley-Interscience, New York, 1997.
[19] M.R.P. Kurup, S.V. Chandra, K. Muraleedharan, J. Therm. Anal. Calorim. 61 (2000) 909–914.
[20] D. Rehder, Inorg. Chem. Commun. 6 (2003) 604–617.
[21] D.N. Sathyanarayana, Vibrational Spectroscopy, New Age International, New Delhi, 2004.
[22] T.A. Reena, E.B. Seena, M.R.P. Kurup, Polyhedron 27 (2008) 1825–1831.
[23] L. Sacconi, G. Speroni, J. Am. Chem. Soc. 87 (1965) 1302–1306.
[24] R.P. John, A. Sreekanth, V. Rajakannan, T.A. Ajith, M.R.P. Kurup, Polyhedron 23 (2004) 2549–2559.
[25] M. Joseph, M. Kuriakose, M.R.P. Kurup, E. Suresh, A. Kishore, G. Bhat, Polyhedron 25 (2006) 61–70.
[26] A.H. Maki, B.R. McGarvey, J. Chem. Phys. 29 (1958) 31–35.
[27] J.R. Wasson, C. Trapp, J. Phys. Chem. 73 (1969) 3763–3772.
[28] B.N. Figgis, Introduction to Ligand Fields, Interscience, NewYork, 1996.
[29] B.J. Hathaway, in: G. Wilkinson, R.D. Gillard, J.A. Mc, Cleverty (Eds.), Comprehensive Coordination Chemistry, vol. 5, Pergamon, Oxford, 1987.
[30] P.F. Rapheal, E. Manoj, M.R.P. Kurup, Polyhedron 26 (2007) 818–828.
[31] V. Philip, V. Suni, M.R.P. Kurup, M. Nethaji, Spectrochim. Acta A 64 (2006) 171–177.
[32] B. Bleany, R.S. Rubins, Proc. Phys. Soc. Lond. 77 (1961) 103–112.
[33] W. Linert, E. Renz, R. Boca, J. Coord. Chem. 40 (1996) 293–309.
[34] R. Singh, I.S. Ahuja, C.L. Yadava, Polyhedron 1 (1981) 327–330.
[35] C.H. Collins, P.M. Lyne, Microbiological Methods, University Park Press, Baltimore, 1970.
[36] S.K. Sengupta, O.P. Pandey, B.K. Srivastava, V.K. Sharma, Transit. Met. Chem. 23 (1998) 349–353.
[37] Z.H. Abd El-Wahab, M.M. Mashaly, A.A. Salman, B.A. El-Shetary, A.A. Faheim, Spectrochim. Acta A 60 (2004) 2861–2873.